LONG TERM ADMINISTRATION OF PIRFENIDONE IMPROVES CARDIAC FUNCTION IN *MDX* MICE

Christel van Erp, BSc, Nicole G Irwin, BSc, Andrew J Hoey, PhD

Centre for Systems Biology
Faculty of Sciences
University of Southern Queensland
Toowoomba
Queensland 4350
Australia

Acknowledgements
We acknowledge the assistance of Steve Porter (Intermune) for the provision of pirfenidone and Peter Dunn (Department of Mathematics and Computing, USQ) for statistical advice. This project was supported by funds from the Queensland Muscular Dystrophy Association and Parent Project Muscular Dystrophy.

Corresponding Author
Andrew J Hoey
Centre for Systems Biology
Faculty of Sciences
University of Southern Queensland
Toowoomba Qld 4350
Australia

Email: hoey@usq.edu.au
Ph: +61 746 311 505
Fax: +61 746 311 530

Running Title: Pirfenidone improves cardiac function in *mdx* mice

LONG TERM ADMINISTRATION OF PIRFENIDONE IMPROVES CARDIAC FUNCTION IN *MDX* MICE

ABSTRACT

Duchenne muscular dystrophy, an X-linked recessive neuromuscular disorder due to lack of the protein dystrophin, manifests as progressive muscle degeneration and cardiomyopathy with increased fibrosis. The exact mechanisms involved in fibrosis are unknown, but the cytokine, TGF-β, is a likely mediator. This study tested whether the TGF-β antagonist, pirfenidone, could reduce cardiac fibrosis. Eight-month-old *mdx* mice were treated for 7 months with 0.4%, 0.8%, and 1.2% of pirfenidone in drinking water: untreated water was given to control *mdx* and C57 mice. Mice treated with 0.8% and 1.2% pirfendone had lowered cardiac TGF-β mRNA and improved in vitro cardiac contractility ($P<0.05$) to levels consistent with C57 mice, yet without a change in cardiac stiffness or fibrosis. These results show that the TGF-β antagonist, pirfenidone can improve cardiac function in *mdx* mice, potentially providing a new avenue for developing cardiac therapies for patients with Duchenne muscular dystrophy.

Keywords

Duchenne Muscular Dystrophy, fibrosis, *mdx* mice, pirfenidone, TGF-β

Introduction

Deficiency of dystrophin, due to a mutation in the dystrophin gene on the X-chromosome, is the primary cause of Duchenne muscular dystrophy (DMD). Boys with DMD often exhibit cardiomyopathy in addition to severe respiratory complications, with these two factors being the major contributors to mortality. The incidence of symptomatic cardiomyopathy increases with age, with all patients over 18 years having detectable cardiac disease[23]. The spectrum of disease includes electrocardiographic changes, impaired systolic and diastolic function, and increased fibrosis [10,14,9]. A recent report on survival of DMD patients indicates that heart failure reduces the average life-expectancy significantly[8], so that strategies to reduce the progression of cardiomyopathy and improve cardiac function are necessary to prolong the lifespan of many boys with DMD.

Dystrophin deficiency causes repeated cycles of myocyte degeneration, consequently leading to increased deposition of collagenous extracellular matrix or fibrosis[15,7]. In the heart, in addition to impairing contractility, fibrosis may interfere with impulse conduction and rhythm[10]. The precise mechanisms causing fibrosis are unknown, although profibrotic cytokines such as transforming growth factor-β (TGF-β) are likely candidates.

TGF-β is a pleiotropic cytokine that plays an important role in inflammation as well as wound and tissue repair[25]. This cytokine is expressed at high levels in the skeletal muscles of patients with DMD, with evidence that its level of expression is related to the degree of muscle fibrosis[3]. Similarly, in the dystrophin deficient *mdx* mouse, fibrosis in the diaphragm is associated with increased TGF-β transcript[13]. Although

high levels of cardiac fibrosis have been reported in 17-month-old *mdx* mice[26], there are no reports of TGF-β levels in dystrophic hearts, at least to our knowledge.

Pirfenidone is an orally active antifibrotic drug that inhibits TGF-β–induced fibroblast growth and collagen synthesis in a range of tissues and disease models. Pirfenidone has shown positive results in double-blind, randomized, controlled clinical trials for interstitial pulmonary fibrosis and has received orphan drug status in Europe and the United States for treatment of that condition[1]. Pirfenidone has also shown positive results in a range of experimental animal models of disease including reduced pulmonary fibrosis in the bleomycin hamster model[16]; glomerulosclerosis in the FGS/Kist mouse model of renal fibrosis[24]; collagen accumulation in postobstructive models of kidney fibrosis in rats[28,29]; and dimethylnitrosamine (DMN)-induced hepatic fibrosis in male Wistar King A rats[31]. Likewise in streptozotocin-induced diabetic rats, pirfenidone reversed cardiac and renal fibrosis, without normalizing cardiac contractility or renal function[19]. In this animal model, pirfenidone decreased fibrosis despite not increasing the rate of pressure development, but the underlying impairment of contractility in this disease state is not solely related to the increase in fibrosis but also to marked changes in calcium handling[33]. In the *mdx* mouse the basis for impaired cardiac contractility has not been clearly delineated and it is therefore possible that a decrease in fibrosis may improve contractility.

As the antifibrotic action of pirfenidone has been demonstrated in several animal models of fibrosis in different organs including heart, lung, kidney, and liver, we tested whether administration of pirfenidone would elicit an antifibrotic action on

cardiac muscle and improve functional responses in *mdx* mice, a model that displays extensive cardiac fibrosis later in life.

Materials and Methods

Treatment Protocol

Male C57BL10ScSn mice (control strain) (C57) and C57BL10ScSn *mdx* mice (*mdx*) were housed at our institutional animal facility. Eight-month-old *mdx* mice were randomized into four groups, with nine mice per group. Three groups of *mdx* mice were treated with pirfenidone (Intermune, Brisbane, CA) in their drinking water at the following concentrations: 0.4, 0.8 and 1.2 g/100 ml. A further group of *mdx* and C57 mice received untreated drinking water and were designated *mdx* and C57 controls. The rate of water consumption was measured and did not differ between the treated and untreated mice. This treatment regime allowed assessment of the drug-induced benefit relative to the untreated *mdx* and C57 mice. All animals were given free access to feed.

Preliminary experiments showed that hearts from 8-to 9-month-old *mdx* mice did not show an elevation in ventricular hydroxyproline content, whereas hearts from 15-month-old *mdx* mice showed both elevated ventricular hydroxyproline and impaired ventricular contractility. Therefore all mice were treated for a total of 7 months allowing a final age of 15 months. All experimental protocols were conducted with the approval of our institutional Animal Ethics Committee, under the guidelines of the National Health and Medical Research Council of Australia.

Langendorff Experiments

Mice at 15 months of age were weighed and anaesthetized with sodium pentobarbital (Nembutal, Boehringer Ingelheim, Artarmon, NSW, Australia) at 70 mg/kg

administered intraperitoneally. A thoracotomy was performed and hearts were rapidly excised into modified Krebs-Henseleit buffer containing (mM): NaCl, 119; $NaHCO_3$, 22; KCl, 4.7; KH_2PO_4, 1.2; $CaCl_2$, 2.5; $MgSO_4$, 1.2; glucose, 11; Na-pyruvate, 1 and EDTA, 0.5 containing 10 mM 2,3-butanedione monoxime (temperature 21°C). The aorta was cannulated via the dorsal root and perfused at a pressure of 80 mmHg with Krebs-Henseleit perfusion buffer maintained at 37°C and bubbled with carbogen (95%O_2-5%CO_2) to ensure a pH of 7.4.

A small polyethylene apical drain was used to vent the left ventricle preventing an accumulation of fluid in this chamber via Thesbian veins. The left atrium was excised and a fluid-filled balloon constructed from polyvinyl chloride plastic film was inserted into the left ventricle via the mitral valve for the measurement of left ventricular function. The left ventricular function was recorded via a MLT844 physiological pressure transducer (ADInstruments, Castle Hill, NSW, Australia) linked to a PowerLab recording system (ADInstruments). Coronary flow was regulated via a ML175 STH Pump Controller (ADInstruments).

Hearts with a coronary flow greater than 5 ml/min, indicating an aortic tear or aortic valve rupture, were to be excluded from the experimental analysis; only one mouse reached this exclusion criteria. Data were recorded using Chart 4.1.1 software (ADInstruments) to calculate end-systolic pressure (ESP) and end-diastolic pressure (EDP), developed pressure and relaxation over time (±dP/dt), and heart rate. Fluid temperature was measured via a thermometer at the entry of the aortic cannula, and temperatures were maintained at 37.3°C.

Hearts were paced at 420 bpm via a Grass S48 stimulator (West Warwick, RI) and a silver wire embedded into the left ventricle and grounded using an electrode attached to the cannula. The balloon was inflated to an EDP between 0 and 5 mmHg and the heart was then equilibrated for 10 minutes at this pressure. Following this equilibration period, the EDP was measured for 30 seconds at each of the following increments: 0, 5, 10, 15, 20 and 30 mmHg. Myocardial stiffness was defined by the stiffness constant (κ, dimensionless), that is, the slope of the linear relationship between the tangent elastic modulus (E, dyne/cm^2) and stress (σ, dyne/cm^2) as described in detail elsewhere[21].

At cessation of the in vitro experiments, the right atrium, right ventricle, and left ventricle plus septum were separated and weighed. The left ventricle plus septum was bisected transversely with the superior portion stored for histology. Half of the remainder was snap frozen in liquid nitrogen and stored at -80°C for subsequent hydroxyproline assays and the other half was stored in RNA*later* (Ambion, Austin, TX) for subsequent determination of TGF-β mRNA levels.

Hydroxyproline Measurements

Hydroxyproline (HP) assays were used as a measure of collagen content. The frozen left ventricular section was weighed and placed in a sealed tube containing 6 M HCl. The following protocol has been described previously in detail[30]. Briefly, the tissue was hydrolyzed overnight at 110°C before being dried using low heat (50°C) and filtered air under pressure. The dried sample was reconstituted with distilled water and Chloramine T reagent was added to each sample. The oxidation step was then allowed to progress for 20 minutes before Ehrlich's reagent was added. The samples

were subsequently incubated at 60°C in a shaking water bath for 20 minutes to allow the chromophore to develop. Values are expressed as μg HP/mg of wet tissue weight. Absorbance was read at 550 nm and HP content was calculated from a standard curve.

Histology

The superior ventricular sections were fixed in Telly's fixative (70% ethanol, 37% formaldehyde and glacial acetic acid) for 3 days, modified Bouin's solution (saturated picric acid, 37% formaldehyde and glacial acetic acid) for 1 day and 70% ethanol before the muscles were embedded in paraffin wax. Sections of 10-μm thickness were cut and placed on Polysine glass slides and stained using the collagen selective stain, 0.1% wt/vol picrosirius red solution (Sirius Red F3B, Chroma Dyes, in saturated picric acid). Slides were left in 0.2% phosphomolybdic acid for 5 minutes, then washed, stained in picrosirius red for 90 minutes and then placed in 1 mM HCl for 2 minutes. Slides were then placed in 70% ethanol for 30 seconds and coverslipped using Depex.

Stained muscle sections were viewed blinded to the strain and treatment of the mouse using a Nikon Eclipse E600 epifluorescence microscope and 200X magnification. Images were captured with a cooled charge-coupled device (CCD) digital camera (Micropublisher 5.0, QImaging, Burnaby, Canada). Picrosirius red-stained cardiac sections were viewed under polarized light to determine the ratio of type I and type III collagen[17]. The automated red:green color separation and phase analysis module within AnalySIS software (Soft Imaging System, GmbH, Münster, Germany) were used to calculate the area of each collagen subtype within each field of view and to remove operator bias. To determine an average percentage of collagen in each left

ventricle, the total collagen of the type I and type III was calculated from two endocardial and three epicardial regions of the left ventricle.

TGF-β mRNA Measurements

RNA*later* treated frozen samples were cut into 6-µm sections and total RNA extracted with an RNAqueous Kit (Ambion). All samples were DNase treated with Turbo DNA-free (Ambion) prior to reverse transcriptase-polymerase chain reaction (RT-PCR) and screened for genomic DNA. RNA was quantified using Quant-it Ribogreen RNA Assay Kit (Molecular Probes; Invitrogen, Eugene, OR). Relative RT-PCR was carried out with 100 pg of total RNA as the starting material for 26 cycles of amplification in the Titan One-Tube RT-PCR system (Roche Molecular Biochemicals, Mannheim, Germany). TGF-β was amplified with the following primers: forward, TGF-β 1446F 5'-TGAGTGGCTGTCTTTTGACG-3'; reverse, TGF-β 1738R 5'-TCTCTGTGGAGCTGAAGCAA-3'. β-actin was co-amplified as an internal control using the following primers: forward, β-actin F561 5'-CACACTGTGCCCATCTACGA-3'; reverse, β-actin R688 5'-GTGGTGGTGAAGCTGTAG-3'.

To determine specificity, all sequences were compared with Genbank Blast (www.ncbi.nlm.nih.gov). TGF-β and β-actin primers were used at a concentration of 10 µM and 20 µM, respectively. Optimal magnesium chloride concentration was 1.0 mM, with all other reaction components added as per manufacturer's instructions. Multiplex reactions were carried out on a ThermoHybaid PCR Express (Integrated Sciences, Sydney, NSW, Australia). A first cycle of 48^{o}C for 30 minutes was undertaken for cDNA synthesis. An initial denaturation step of 94^{o}C for 2 minutes

was performed, followed by a touch-down PCR protocol as described below: 30 seconds at 94^{o}C, 1 minute at 62^{o}C, 2 minutes at 72^{o}C for 2 cycles; 30 seconds at 94^{o}C, 1 minute at 60^{o}C and 2 minutes at 72^{o}C for 2 cycles; 30 seconds at 94^{o}C, 1 minute at 58^{o}C and 2 minutes at 72^{o}C for 2 cycles; 30 seconds at 94^{o}C, 1 minute at 56^{o}C and 2 minutes at 72^{o}C for 20 cycles. A final extension was performed at 72^{o}C for 5 minutes. Cycling parameters were optimized to ensure exponential phase amplification of TGF-β and β-actin. PCR products were run on a 2% agarose gel in Tris Acetate EDTA buffer and visualised with ethidium bromide. A PCR DNA ladder (New England Biolabs, Ipswich, MA) was run on each gel to confirm the expected molecular weight of the amplification product. Results were analysed using Scion Image Software beta 4.0.2 (www.scioncorp.com) and TGF-β product normalized by comparison to the β -actin internal control product.

Statistical Analysis

Data are presented as mean ± SEM, and comparisons were made using ANOVA. Differences between groups were determined post hoc using Tukeys HSD test if variances were shown to be equal or Games-Howell post hoc test if variance was unequal. A value of $P<0.05$ was considered statistically significant.

Results

Cardiac Structure and Function

Mdx mice had impaired cardiac function relative to age and-sex-matched C57 mice, as evidenced by a reduction of 26% in left ventricular developed pressure ($P<0.001$), 29% in +dP/dt ($P<0.01$) and 21% in –dP/dt ($P<0.01$; Fig. 1). In contrast, *mdx* mice treated with 0.8% and 1.2% pirfenidone showed a significantly improved cardiac contractility with developed pressure increased in *mdx* mice to a level commensurate with that measured in hearts from C57 mice. Similarly, +dP/dt was improved in *mdx* mice treated with 0.8% pirfenidone ($P<0.01$), and was close to significance in mice treated with 0.4% ($P<0.07$) and 1.2% ($P<0.08$). Associated with this -dP/dt was also improved with 0.8% pirfenidone ($P<0.06$), with this reaching significance in 1.2% pirfenidone ($P<0.05$) compared to untreated *mdx* mice, resulting in values similar to those measured in hearts from C57 mice. There were no significant differences in coronary flow or diastolic stiffness between the untreated *mdx* and C57 mice or between hearts from untreated and pirfenidone treated *mdx* mice (Table 1).

To determine whether changes in contractility were related to reduced fibrosis, cardiac collagen content was measured. Hydroxyproline content was higher in the left ventricles of untreated *mdx* mice than C57 control mice ($P<0.01$) but pirfenidone did not reduce hydroxyproline content (Fig. 2). These findings were reinforced by analysis of picrosirius red-stained left ventricular sections, which showed that total collagen was increased in *mdx* mice ($P<0.05$) but unaltered by pirfenidone treatment (Fig. 3). The ratio of type I:III collagen was not different between treated and untreated *mdx* mice, nor was a ratio difference evident between *mdx* and C57 mice (Table 1).

TGF-β mRNA expression

To confirm that pirfenidone lowered TGF-β mRNA expression, RT-PCR experiments were undertaken. The quantity of TGF-β mRNA was not different between *mdx* and C57 mice. Pirfenidone treatment at concentrations of 0.8 and 1.2% decreased the TGF-β mRNA levels significantly ($P<0.01$) compared to both the C57 and untreated *mdx* mice. (Fig. 4)

Discussion

The aged *mdx* mouse exhibits several cardiomyopathic features similar to those observed in DMD cardiomyopathy. We assessed ventricular function in *mdx* mice older than 12 months of age and found evidence of reduced ventricular contractility, rate of pressure development, and rate of relaxation in the *mdx* mouse heart. These features correspond to the cardiac features in boys with DMD where there is also increased fibrosis with reduced systolic and diastolic function[4]. The *mdx* mouse ventricles also exhibit significantly elevated collagen content evident by picrosirius red staining, as reported previously,[26] with no change evident in collagen I:III ratio. Using hydroxyproline assays, this increase in collagen has been further verified. Interestingly, despite the increased cardiac collagen, there was no difference in diastolic stiffness. This was unexpected although a similar finding was reported in younger *mdx* mice[32]. Because different collagen subtypes contribute to stiffness, we assessed the ratio of subtype I and III, but found no difference between *mdx* and C57 mice. The lack of increased stiffness in older *mdx* mice suggests low levels of crosslinking or other compensatory changes in the *mdx* mouse to allay the effects of the increased collagen[5,2].

We investigated the effect of pirfenidone in *mdx* mice and the long-term efficacy study with pirfenidone in animals. The results show that 0.8% and 1.2% pirfenidone reduced TGF-β mRNA levels associated with a marked improvement in cardiac function, yet without a reduction of ventricular collagen content. Evidence of improved cardiac function included increased ventricular developed pressure, +dP/dt

and -dP/dt. Importantly, these functional parameters improved to values that were not significantly different to values measured in C57 mice.

While treatment with pirfenidone has reproducibly shown antifibrotic effects in a range of acutely induced fibrosis in tissues including lungs, liver, kidneys and heart, no antifibrotic effect was evident in this study. Many animal studies investigating the action of pirfenidone have utilized rats or hamsters in their research, but because mice have a higher relative metabolic rate, a range of doses was tested. Therefore, in our study mice received a range of doses from 0.4% to 1.2% in water (equating to approximately 0.4-1.2 g/kg) in contrast to previous studies in rats and hamsters that utilized lower doses of pirfenidone at a dose of 0.4 to 0.5% in food (equating to approximately 0.3-0.7 g/kg). Therefore, the lack of anti-fibrotic effects in this study are unlikely to be due to an insufficient dosage, particularly as 0.8% and 1.2% pirfenidone both reduced TGF-β mRNA even though no concurrent reduction occurred in fibrosis.

It can be hypothesized that the lack of observed antifibrotic effect with pirfenidone treatment is due to either: (1) fibrosis in *mdx* mouse hearts increasing with age due to impairment of collagen degradation in addition to increased collagen synthesis; or (2) advanced establishment of profibrotic pathways in the *mdx* mouse hearts by 8 months of age, which was when pirfenidone treatment commenced.

In support of the first possibility, recent data obtained from diaphragms of *mdx* mice shows extensive and progressive development of fibrosis from early in life with increased procollagen 1 mRNA evident from 6 weeks of age. However, by 12 weeks

of age, no difference in procollagen 1 mRNA was evident between *mdx* and C57 mouse diaphragms, suggesting reduced degradation rather than increased fibrosis is the basis of increased collagen content[13]. This, in turn, would reduce the likelihood of antifibrotic benefits of pirfenidone, especially in mice at 15 months of age.

In support of the second possibility, the *mdx* mouse undergoes an acute inflammatory response early in life with increased expression of cytokines including TNF-α and TGF-β, which may lay the foundation for pathways leading to increased fibrosis. For example, TGF-β expression is elevated at 6 and 9 weeks of age, but not at 12 weeks[13], suggesting profibrotic pathways are initiated early. This would also explain why TGF-β mRNA levels were not different in the hearts of the 15-month-old *mdx* mice compared to the C57 mice. Treating mice older than 6 to 9 weeks with pirfenidone, which acts to inhibit TGF-β expression, is thus unlikely to be effective. Further support for the need to intervene early in the inflammatory process is that treatment of hamsters with pirfenidone for 3 days before amiodarone-induction of pulmonary fibrosis prevented subsequent fibrosis when measured at its peak, 21 days later. In contrast, delaying pirfenidone treatment until 7 days post-amiodarone treatment did not protect against fibrosis developing. This lack of antifibrotic effect occurred despite the capacity of pirfenidone to reduce TGF-β mRNA, although to a lesser extent than the reduction that was measured with pirfenidone administration prior to amiodarone-induction of pulmonary fibrosis[6].

The current study shows that long-term treatment causes a clear improvement in cardiac function, in contrast to previous studies. Acute rat models of cardiovascular diseases, deoxycorticosterone-acetate (DOCA)-salt and streptozotocin (STZ)-induced

diabetes did not show improved cardiac contractility after pirfenidone treatment for 2 weeks at doses that were effective at preventing increased fibrosis and diastolic stiffness[19,20]. These differences may be due to species differences or duration of treatment.

Recent studies have shown that pirfenidone also modifies numerous other cytokines, including inhibition of TNF-α, interferon-γ, and interleukin-6, while enhancing synthesis of the anti-inflammatory cytokine interleukin-10 in mouse and rat models of endotoxic shock[22,18]. Pirfenidone may also scavenge reactive oxygen species[12] which are elevated and cause detrimental effects in *mdx* mouse tissues[27]. Pirfenidone's capacity to scavenge reactive oxygen species and lower levels of H_2O_2, OH^- and O_2^- may be a basis of improved cardiac function. Furthermore, since it is increasingly recognized that cardiomyopathy is a complex neurohumoral disorder involving many inflammatory cytokines, it is unlikely that inhibition of a single cytokine will be useful in the treatment of cardiomyopathy[11]. Whether pirfenidone acts solely through inhibition of TGF-β or through inhibition of a range of inflammatory cytokines, remains to be resolved.

In conclusion, long-term treatment with pirfenidone improves cardiac function in *mdx* mice, but does not prevent fibrosis when treatment is commenced later in the lifespan. The higher pirfenidone doses (0.8% and 1.2%) decreased TGF-β RNA expression and these same doses caused an increase in cardiac function. It appears that the administration of pirfenidone at 0.8% is the optimum dose for *mdx* mice to produce the most significant cardiac function improvement. Further studies should investigate the actions of pirfenidone during the acute inflammatory stage of the disease to

determine if earlier administration will inhibit upregulation of inflammatory or profibrotic cytokines to improve both function and prevent fibrosis, both of which would be beneficial in treatment of DMD.

Abbreviations

DMD,	Duchenne Muscular Dystrophy
+dP/dt,	rate of pressure development
-dP/dt,	rate of relaxation
EDP,	end-diastolic pressure
ESP,	end-systolic pressure
HP,	hydroxyproline
RT-PCR,	reverse transcriptase-polymerase chain reaction
TGF-β,	Transforming growth factor-beta

References

1. Antoniu SA. Pirfenidone for the treatment of idiopathic pulmonary fibrosis: therapeutic potential prompts further investigation. Expert Opin Investig Drugs 2005;14:1443-1447.
2. Badenhorst D, Maseko M, Tsotetsi OJ, Naidoo A, Brooksbank R, Norton GR, Woodiwiss AJ. Cross-linking influences the impact of quantitative changes in myocardial collagen on cardiac stiffness and remodelling in hypertension in rats. Cardiovasc Res 2003;57:632-641.
3. Bernasconi P, Torchiana E, Confalonieri P, Brugnoni R, Barresi R, Mora M, Cornelio F, Morandi L, Mantegazza R. Expression of transforming growth factor-beta 1 in dystrophic patient muscles correlates with fibrosis. Pathogenetic role of a fibrogenic cytokine. J Clin Invest 1995;96:1137-1144.
4. Brockmeier K, Schmitz L, von Moers A, Koch H, Vogel M, Bein G. X-chromosomal (p21) muscular dystrophy and left ventricular diastolic and systolic function. Pediatr Cardiol 1998;19:139-144.
5. Bronzwaer JG, Paulus WJ. Matrix, cytoskeleton, or myofilaments: which one to blame for diastolic left ventricular dysfunction? Prog Cardiovasc Dis 2005;47:276-284.
6. Card JW, Racz WJ, Brien JF, Margolin SB, Massey TE. Differential effects of pirfenidone on acute pulmonary injury and ensuing fibrosis in the hamster model of amiodarone-induced pulmonary toxicity. Toxicol Sci 2003;75:169-180.

7. Chen YW, Nagaraju K, Bakay M, McIntyre O, Rawat R, Shi R, Hoffman EP. Early onset of inflammation and later involvement of TGF{beta} in Duchenne muscular dystrophy. Neurology 2005;65:826-834.

8. Eagle M, Baudouin SV, Chandler C, Giddings DR, Bullock R, Bushby K. Survival in Duchenne muscular dystrophy: improvements in life expectancy since 1967 and the impact of home nocturnal ventilation. Neuromuscul Disord 2002;12:926-929.

9. Farah MG, Evans EB, Vignos PJ, Jr. Echocardiographic evaluation of left ventricular function in Duchenne's muscular dystrophy. Am J Med 1980;69:248-254.

10. Finsterer J, Stollberger C. The heart in human dystrophinopathies. Cardiology 2003;99:1-19.

11. Fonarow GC. Pathogenesis and treatment of cardiomyopathy. Adv Intern Med 2001;47:1-45.

12. Giri SN, Leonard S, Shi X, Margolin SB, Vallyathan V. Effects of pirfenidone on the generation of reactive oxygen species in vitro. J Environ Pathol Toxicol Oncol 1999;18:169-177.

13. Gosselin LE, Williams JE, Deering M, Brazeau D, Koury S, Martinez DA. Localization and early time course of TGF-beta 1 mRNA expression in dystrophic muscle. Muscle Nerve 2004;30:645-653.

14. Hoogerwaard EM, van der Wouw PA, Wilde AA, Bakker E, Ippel PF, Oosterwijk JC, Majoor-Krakauer DF, van Essen AJ, Leschot NJ, de Visser M. Cardiac involvement in carriers of Duchenne and Becker muscular dystrophy. Neuromuscul Disord 1999;9:347-351.

15. Ionasescu V, Ionasescu R. Increased collagen synthesis by Duchenne myogenic clones. J Neurol Sci 1982;54:79-87.

16. Iyer SN, Gurujeyalakshmi G, Giri SN. Effects of pirfenidone on transforming growth factor-beta gene expression at the transcriptional level in bleomycin hamster model of lung fibrosis. J Pharmacol Exp Ther 1999;291:367-373.

17. Junqueira LC, Cossermelli W, Brentani R. Differential staining of collagens type I, II and III by Sirius Red and polarization microscopy. Arch Histol Jpn 1978;41:267-274.

18. Kaibori M, Yanagida H, Yokoigawa N, Hijikawa T, Kwon AH, Okumura T, Kamiyama Y. Effects of pirfenidone on endotoxin-induced liver injury after partial hepatectomy in rats. Transplant Proc 2004;36:1975-1976.

19. Miric G, Dallemagne C, Endre Z, Margolin S, Taylor SM, Brown L. Reversal of cardiac and renal fibrosis by pirfenidone and spironolactone in streptozotocin-diabetic rats. Br J Pharmacol 2001;133:687-694.

20. Mirkovic S, Seymour AM, Fenning A, Strachan A, Margolin SB, Taylor SM, Brown L. Attenuation of cardiac fibrosis by pirfenidone and amiloride in DOCA-salt hypertensive rats. Br J Pharmacol 2002;135:961-968.

21. Mirsky I, Parmley WW. Assessment of passive elastic stiffness for isolated heart muscle and the intact heart. Circ Res 1973;33:233-243.

22. Nakazato H, Oku H, Yamane S, Tsuruta Y, Suzuki R. A novel anti-fibrotic agent pirfenidone suppresses tumor necrosis factor-alpha at the translational level. Eur J Pharmacol 2002;446:177-185.

23. Nigro G, Comi LI, Politano L, Bain RJ. The incidence and evolution of cardiomyopathy in Duchenne muscular dystrophy. Int J Cardiol 1990;26:271-277.

24. Park HS, Bao L, Kim YJ, Cho IH, Lee CH, Hyun BH, Margolin SB, Park YH. Pirfenidone suppressed the development of glomerulosclerosis in the FGS/Kist mouse. J Korean Med Sci 2003;18:527-533.

25. Passerini L, Bernasconi P, Baggi F, Confalonieri P, Cozzi F, Cornelio F, Mantegazza R. Fibrogenic cytokines and extent of fibrosis in muscle of dogs with X-linked golden retriever muscular dystrophy. Neuromuscul Disord 2002;12:828-835.

26. Quinlan JG, Hahn HS, Wong BL, Lorenz JN, Wenisch AS, Levin LS. Evolution of the mdx mouse cardiomyopathy: physiological and morphological findings. Neuromuscul Disord 2004;14:491-496.

27. Rando TA, Disatnik MH, Yu Y, Franco A. Muscle cells from mdx mice have an increased susceptibility to oxidative stress. Neuromuscul Disord 1998;8:14-21.

28. Shimizu T, Fukagawa M, Kuroda T, Hata S, Iwasaki Y, Nemoto M, Shirai K, Yamauchi S, Margolin SB, Shimizu F, Kurokawa K. Pirfenidone prevents collagen accumulation in the remnant kidney in rats with partial nephrectomy. Kidney Int Suppl 1997;63:S239-243.

29. Shimizu T, Kuroda T, Hata S, Fukagawa M, Margolin SB, Kurokawa K. Pirfenidone improves renal function and fibrosis in the post-obstructed kidney. Kidney Int 1998;54:99-109.

30. Stegemann H, Stalder K. Determination of hydroxyproline. Clin Chim Acta 1967;18:267-273.

31. Tada S, Nakamuta M, Enjoji M, Sugimoto R, Iwamoto H, Kato M, Nakashima Y, Nawata H. Pirfenidone inhibits dimethylnitrosamine-induced hepatic fibrosis in rats. Clin Exp Pharmacol Physiol 2001;28:522-527.

32. Wilding JR, Schneider JE, Sang AE, Davies KE, Neubauer S, Clarke K. Dystrophin- and MLP-deficient mouse hearts: marked differences in morphology and function, but similar accumulation of cytoskeletal proteins. Faseb J 2005;19:79-81.

33. Yaras N, Ugur M, Ozdemir S, Gurdal H, Purali N, Lacampagne A, Vassort G, Turan B. Effects of diabetes on ryanodine receptor Ca release channel (RyR2) and Ca2+ homeostasis in rat heart. Diabetes 2005;54:3082-3088.

Figure Legends

Figure 1: Cardiac function from control *mdx* and C57 mice and the pirfenidone-treated *mdx* mice. Left ventricular developed pressure (A); Rate of pressure development (+dP/dt) (B); and rate of relaxation (-dP/dt) (C). Untreated *mdx* had a lower function relative to C57 mice whereas 0.8% and 1.2% pirfenidone treatment improved function to levels similar to those measured in hearts from C57 mice. $^{++}P<0.01$, $^{+++}P<0.001$ (C57 vs. *mdx* control mice) $*P<0.05$, $**P<0.01$ (pirfenidone treated *mdx* vs. control *mdx* mice).

Figure 2: Left ventricular hydroxyproline content from control *mdx* and C57 mice and pirfenidone-treated *mdx* mice. Control and treated *mdx* mice had significantly higher hydroxyproline content than C57 mice. $^{+}P<0.05$; C57 vs. *mdx* control.

Figure 3: Left ventricular sections of control *mdx* and C57 and pirfenidone treated *mdx* mice. Total collagen was higher in untreated *mdx* mice and was unaltered by pirfenidone treatment. Viewed under polarized light, magnification: X200. Areas stained red/yellow indicate presence of collagen I and areas stained green indicate presence of collagen III. The rectangle in the C57 photomicrograph is shown enlarged in the image to the right. The arrow shows green birefringence.

Figure 4: Relative RT-PCR quantification of TGF-β normalized to β-actin expression. Relative RT-PCR gel of TGF-β (293 bp) and β-actin (127 bp) (A). Quantified TGF-β expression relative to β-actin (B). Pirfenidone at doses of 0.8% and 1.2% inhibited

TGF-β mRNA expression. significantly compared to both the C57 and untreated *mdx* mice. $^{++}P<0.01$

Table 1: Diastolic stiffness (κ), normalized coronary flow (ml/mg heart weight) and ratio of collagen I:III values for control and pirfenidone treated mice. No significant differences were evident between either strains or treatment groups.

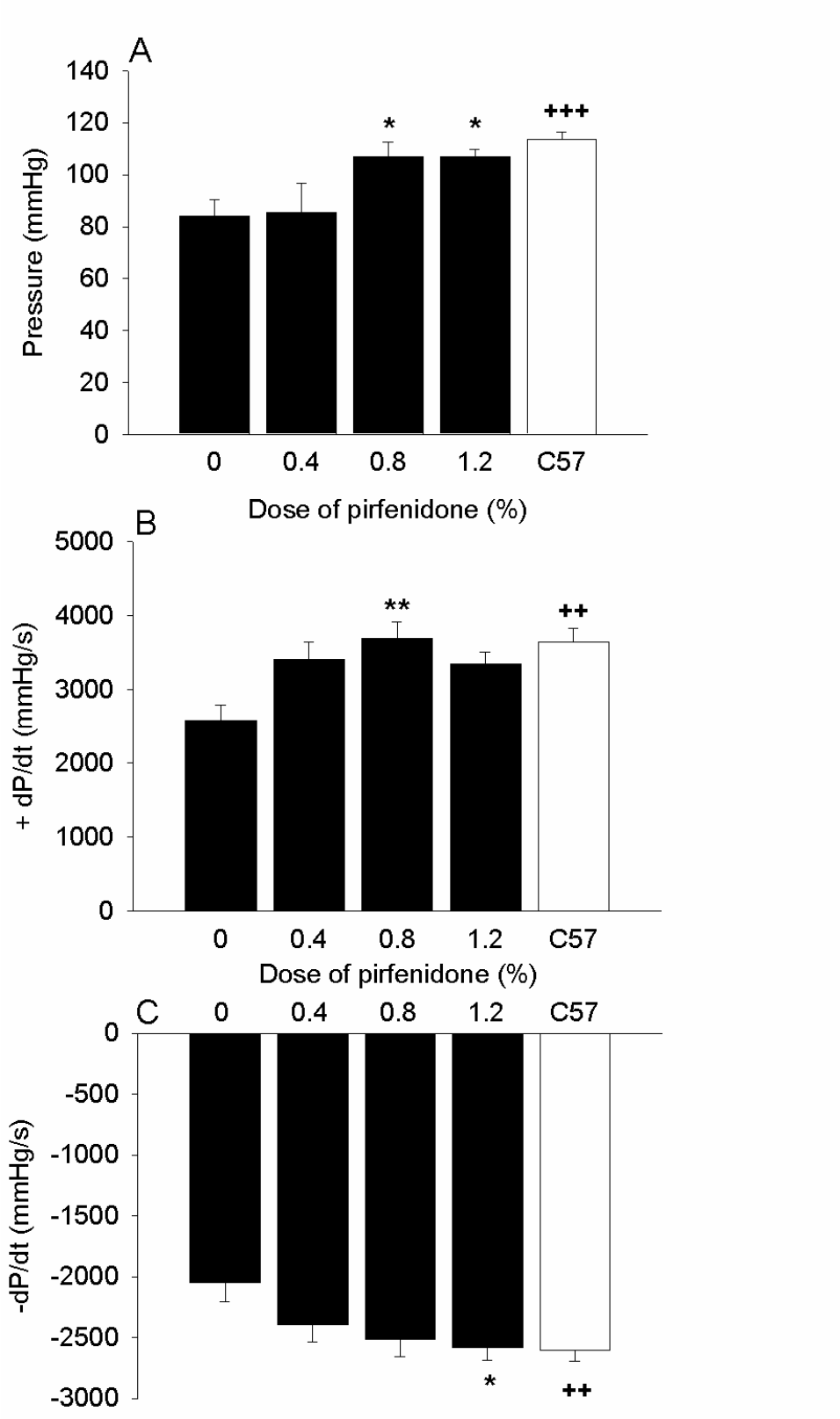
A
Pressure (mmHg)
140
120
100
80
60
40
20
0
*
*
+++
0
0.4
0.8
1.2
C57
Dose of pirfenidone (%)
B
+ dP/dt (mmHg/s)
5000
4000
3000
2000
1000
0
**
++
0
0.4
0.8
1.2
C57
Dose of pirfenidone (%)
C
-dP/dt (mmHg/s)
0
-500
-1000
-1500
-2000
-2500
-3000
0
0.4
0.8
1.2
C57
*
++

Figure 1

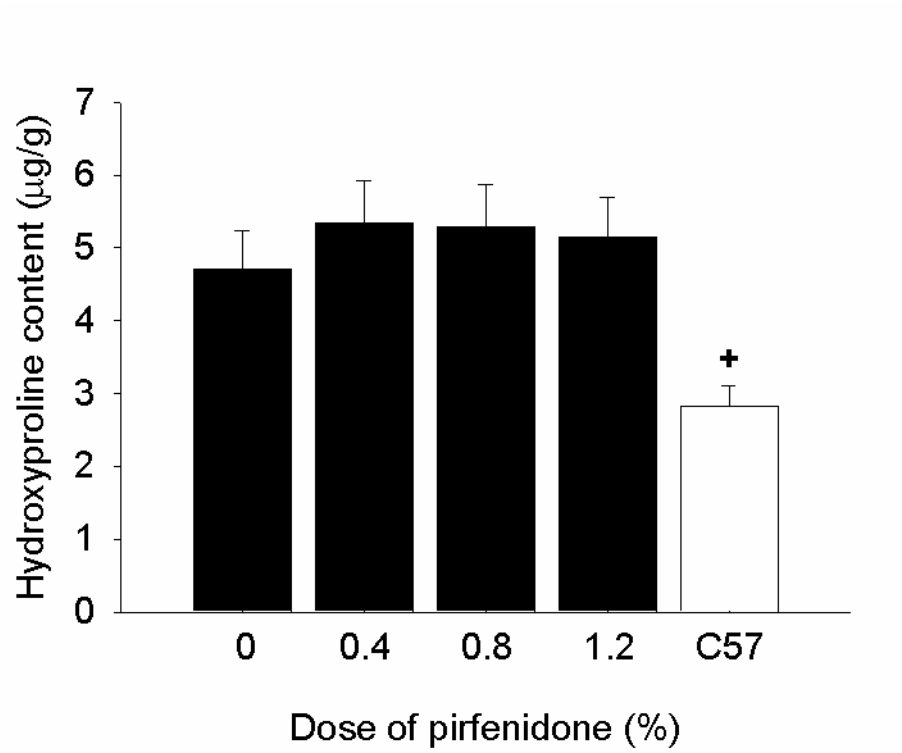
Hydroxyproline content (μg/g)
7
6
5
4
3
2
1
0
+
0
0.4
0.8
1.2
C57
Dose of pirfenidone (%)

Figure 2

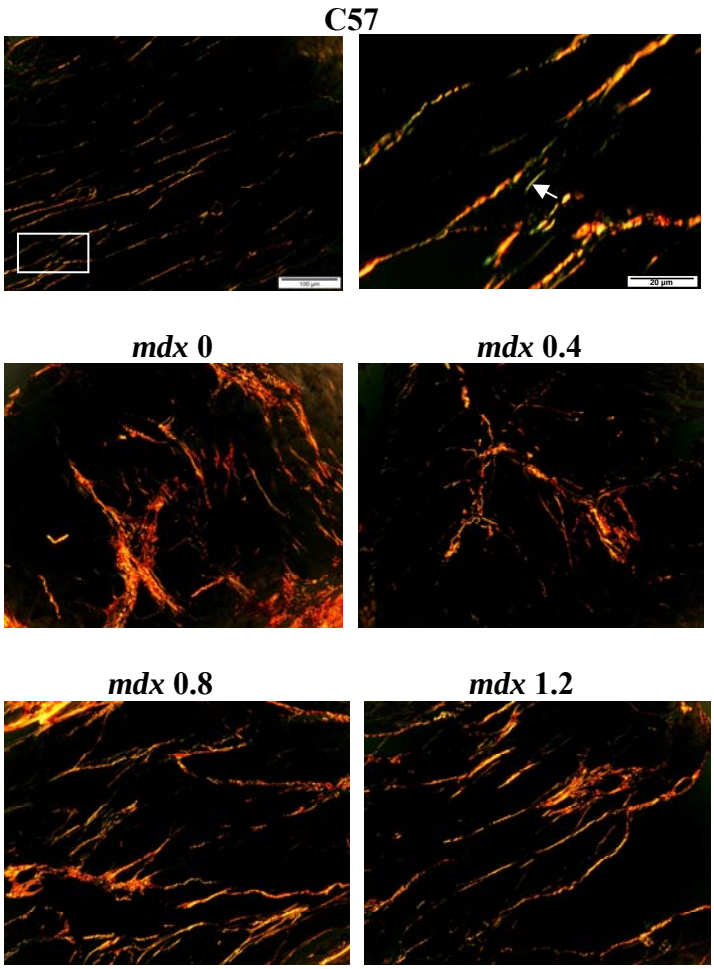

Figure 3

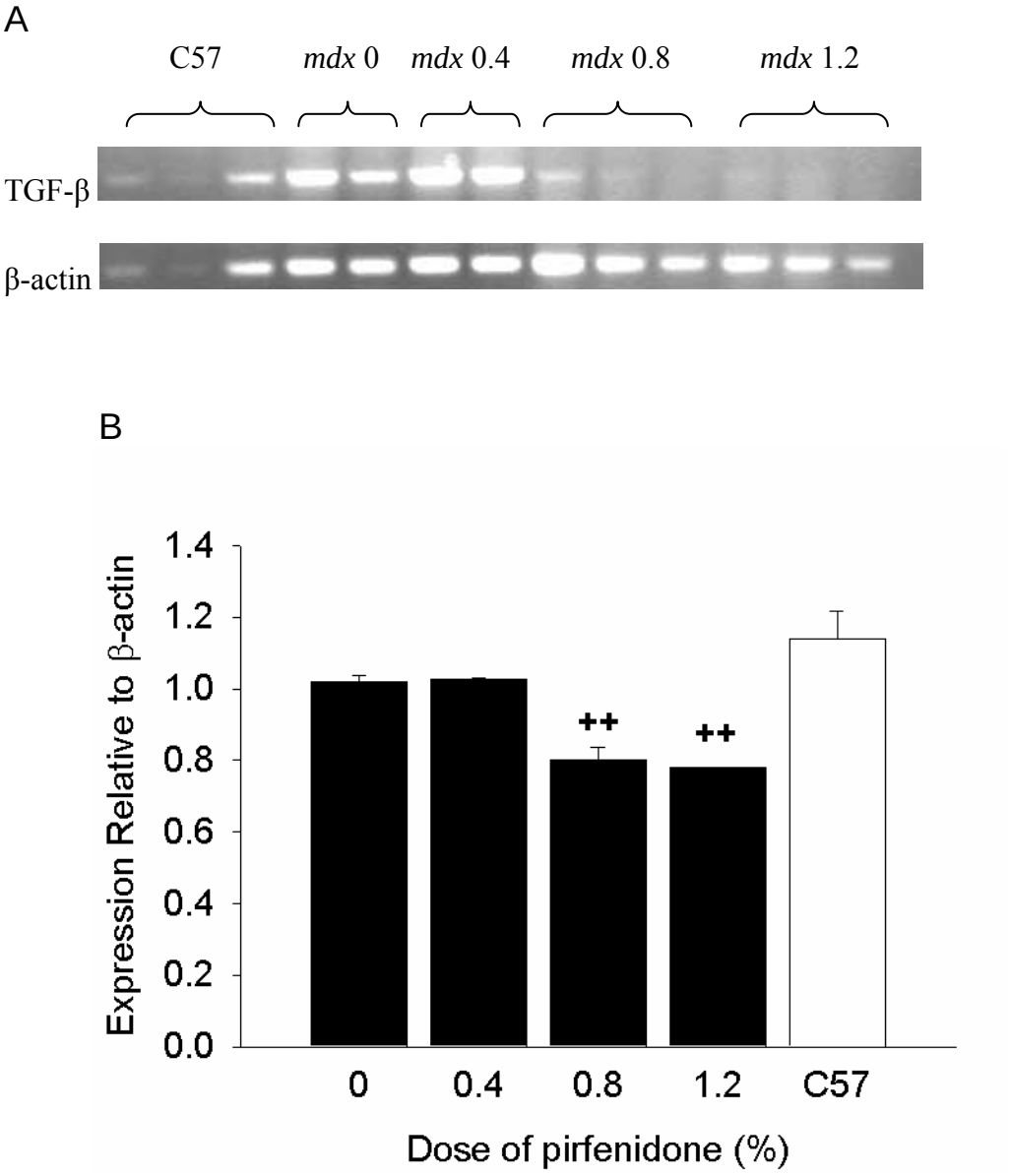
A
C57
mdx 0
mdx 0.4
mdx 0.8
mdx 1.2
TGF-β
β-actin
B
Expression Relative to β-actin
1.4
1.2
1.0
0.8
0.6
0.4
0.2
0.0
++
++
0
0.4
0.8
1.2
C57
Dose of pirfenidone (%)

Figure 4

		***mdx*: Pirfenidone treatment**			
	C57	**0**	**0.4%**	**0.8%**	**1.2%**
Diastolic Stiffness (κ)	32.56±1.29	29.92±2.4	31.34±2.69	33.11±2.13	29.77±2.44
Coronary Flow (ml/mg ht wt)	0.024±0.001	0.024±0.001	0.025±0.002	0.027±0.001	0.024±0.01
Ratio Collagen I:III	2.15±0.14	2.06±0.045	2.30±0.09	2.20±0.1	2.2±0.04

Table 1